

Interaction Transformer for Human Reaction Generation

Baptiste Chopin, Hao Tang, Naima Othberdout, Mohamed Daoudi, *Senior Member, IEEE*, Nicu Sebe, *Senior Member, IEEE*

Abstract—We address the challenging task of human reaction generation which aims to generate a corresponding reaction based on an input action. Most of the existing works do not focus on generating and predicting the reaction and cannot generate the motion when only the action is given as input. To address this limitation, we propose a novel interaction Transformer (InterFormer) consisting of a Transformer network with both temporal and spatial attentions. Specifically, the temporal attention captures the temporal dependencies of the motion of both characters and of their interaction, while the spatial attention learns the dependencies between the different body parts of each character and those which are part of the interaction. Moreover, we propose using graphs to increase the performance of the spatial attention via an interaction distance module that helps focus on nearby joints from both characters. Extensive experiments on the SBU interaction, K3HI, and DuetDance datasets demonstrate the effectiveness of InterFormer. Our method is general and can be used to generate more complex and long-term interactions.

Index Terms—Interaction, Transformer, Human Reaction Generation.

I. INTRODUCTION

Modeling dynamics of human motion is at the core of many applications in computer vision and robotics. Most works on human motion generation ignore human interactions and focus rather on the generation of actions of a single person. In addition, only few works investigating human interaction generation [1] look at the reaction generation problem. What makes human reaction generation a challenging problem is the nonlinearity in the temporal evolution of human motion and the two sources that condition the motion: the action and its corresponding reaction. The first issue arises because human motion is generally performed at varying evolution rates. In other words, a person performing the same activity will go roughly through the same stages but at slightly different rates every time. In addition, as stated by [2], unlike simple actions such as walking or running, complex human interactions such as duet dancing generate highly complex pose sequences

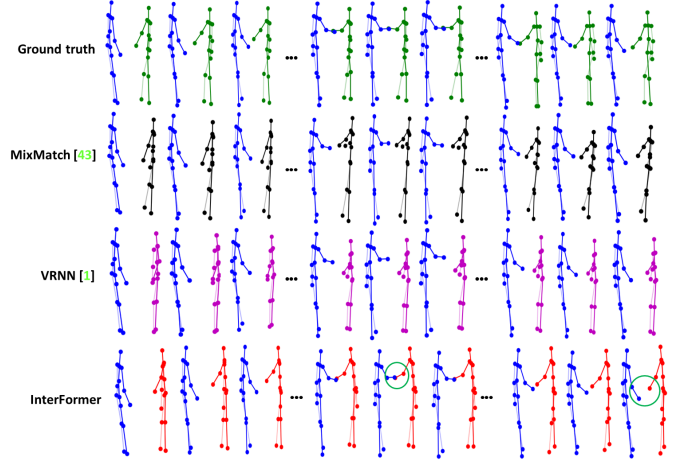


Fig. 1: **Example of reaction generation.** In blue the action motion used as a condition, in other colors the reaction either from the ground truth or generated by the different models. Example from the shaking class of the SBU dataset. Our model generate a more realistic motion than the competing approaches.

operating close to the limit of human kinematics with very low periodicity. The second issue arises because the same action can have a different reaction depending on the interaction context, e.g., when reacting to a punch depending on the position, one can react more or less strongly. These two issues make the generation and the evaluation of reaction challenging. Several questions arise as we try to tackle this challenge. How to translate action to reaction? How to model the long-term sequence? How to represent a complex action-reaction sequence?

Our goal is to learn the reaction from a training sequence of actions and reactions by using Transformer architectures. The breakthroughs from Transformer networks in Natural Language Processing (NLP) domain have sparked great interest in computer vision. Transformer architectures are based on a self-attention mechanism that learns the relationships between elements of a sequence. Unlike recurrent networks that process the elements of the sequence recursively, Transformers can attend to complete sequences thereby are able to learn spatial and temporal relationships making them a good candidate for modeling human motion. In this paper, we propose InterFormer which, with its spatial and temporal attention modules, is able not only to model the spatial and temporal dependencies in the action and in the reaction but also in the interaction between the two humans providing a solution to the two previously mentioned issues. Figure 2 (Left) shows

B. Chopin and N. Othberdout are with Univ. Lille, CNRS, Centrale Lille, UMR 9189 CRISTAL, F-59000 Lille, France. E-mail: {baptiste.chopin,naima.othberdout}@univ-lille.fr

Hao Tang is with the Department of Information Technology and Electrical Engineering, ETH Zurich, Zurich 8092, Switzerland. E-mail: hao.tang@vision.ee.ethz.ch

M. Daoudi is with IMT Nord Europe, Institut Mines-Télécom, Univ. Lille, Centre for Digital Systems, F-59000 Lille, France, and Univ. Lille, CNRS, Centrale Lille, Institut Mines-Télécom, UMR 9189 CRISTAL, F-59000 Lille, France, E-mail: mohamed.daoudi@imt-nord-europe.fr

Nicu Sebe is with the Department of Information Engineering and Computer Science, University of Trento, Trento 38123, Italy. E-mail: nicu-lae.sebe@unitn.it

Manuscript received April 19, 2021; revised August 16, 2021.

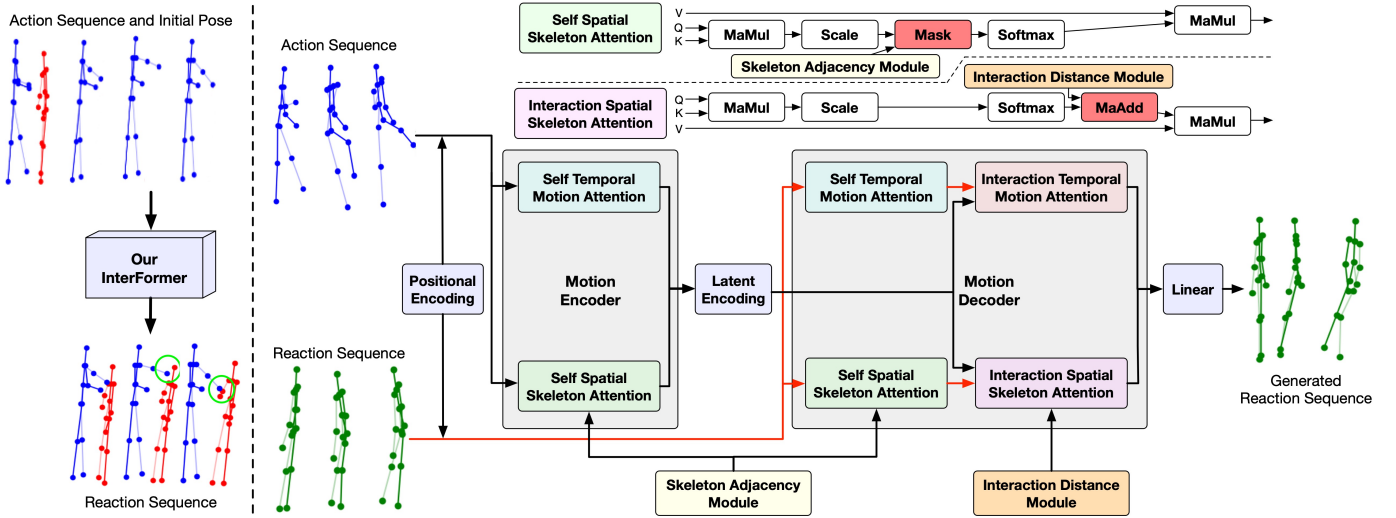


Fig. 2: **Left:** InterFormer during testing: given an action sequence (blue) and the first frame of a reaction sequence (red), we generate the full reaction sequence. We predict one frame at a time based on the previously generated frames. **Right:** Overview of InterFormer during training. The motion encoder takes an action sequence as the input and outputs a latent encoding. The motion decoder takes as inputs the reaction sequence corresponding to the action sequence and the latent encoding from the encoder. The motion decoder outputs a generated reaction sequence. Both encoder and decoder contain several attention modules. **Top Right:** The skeleton adjacency and interaction distance modules interact directly with the spatial attentions.

how our InterFormer can generate a proper reaction sequence (red skeleton) by taking as input an action sequence (blue skeletons) and the initial position of the reaction sequence. Green circles highlight the reaction parts of the motion: the head goes backward in reaction to the punch; the hand is raised as the body continues to move backward to keep its balance. Figure 3 shows a generated reaction from the “shaking hands” class of the SBU dataset. Our method is able to generate a proper motion.

Our major contributions are as follows:

- We propose a novel Interaction Transformer framework for the challenging human reaction generation task. To the best of our knowledge, this is the first Transformer-based work that addresses the problem of human reaction prediction given the action of the interacting skeleton.
- We formulate the reaction generation problem as a translation problem, where we translate a given action of a skeleton to its corresponding reaction such that the entire interaction looks coherent and natural.
- We adopt a graph representation for self-attention to better exploit the skeleton structure while we ignore this representation for computing the attention between the two interacting skeletons. In this case, instead of a graph representation, we exploit the distance between the interacting joints assuming that closer joints involve stronger interaction. By introducing this distance, we provide the prior knowledge that helps to model the interaction.
- While the previous methods for interaction generation address limited and simple short-term interactions, we evaluate our method on the DuetDance dataset that provides more complex and long-term interactions.

II. RELATED WORK

Human Action Generation. Human action recognition and prediction from 3D skeletons is a popular topic [3]–[7]. Inspired by the recent advances in generative models, several works [8]–[11] proposed human action generation models in order to generate a consecutive sequence of human motions. Recently there has been an increase in motion generation based on different modalities, [12] use control signal such as the global trajectory of the person to generate human motion in long term horizons while [13] and [14] generate motion based on speech audio. Meanwhile, others use only knowledge of the past motion which allow them to work in real time but on shorter motion [4], [5], [15]. However, these works only focus on the generation of individual actions. More recently, interaction prediction and generation has also been addressed [1], [2]. For instance, [1] use a multimodal variational recurrent neural network to predict the future motion of both participants in an interaction based on pasts sequences of motion. To complement the existing dataset with interactions [16], [17], different type of complex interaction datasets have also emerged like [18] and their collection of conversational hand motions or triadic interactions [19]. Some works also look at human reaction with other modalities such as walking trajectories [20] or conversational data [21]–[23].

However, there are very few works on human reaction generation. In this paper, we focus on this and propose InterFormer, a novel Transformer architecture. This idea has not been investigated by any other existing work.

Graph Representation has been widely used for 3D classification and segmentation [24], [25], visual question answering [26], human interaction recognition [27], [28]. For instance, [27] proposed a Dyadic Relational Graph Convolutional Network (DR-GCN) for skeleton-based interaction

recognition. When dealing with 3D skeletons, it is natural to use a graph representation as the graph of the skeleton exists physically in the form of segments linking joints. While most works use the graph representation of the skeleton directly as an input, doing so when dealing with interaction leads to losing information. We propose to use the graph as part of the attention module to take advantage of the graph representation without losing the information about the interaction. Experiments show the effectiveness of the proposed InterFormer over existing methods.

Vision Transformers. Transformers were introduced in [29] as a new attention-based building block for machine translation. Because the architecture was powerful and flexible, it was quickly adapted to other natural language processing tasks like language modeling [30], [31]. They also have recently demonstrated good performance on a broad range of tasks such as image generation [32], object detection [33], depth estimation [34], image synthesis [35], and action recognition [28]. Different from these methods, we use a Transformer architecture with temporal and spatial attention for solving the reaction generation task. Generating a reaction responding to an action can be seen as a translation problem: translating from a language “action” to a language “reaction”. The performance of the Transformer on natural language translation tasks and its use of temporal information are a good fit for our task of reaction generation. By adding spatial attention and graph information, we can produce a realistic reaction to an action. To the best of our knowledge, InterFormer is the first Transformer architecture used to solve the problem of human reaction generation.

III. THE PROPOSED INTERACTION TRANSFORMER

Let us consider P_t the positions of k distinct joints at time t . Consequently, an action sequence P of T frames, can be described as a sequence $P=\{P_1, P_2, \dots, P_T\}$, where $P_t \in \mathbb{R}^d$ and $d=3 \times k$, where $P_t=[J_1(t), \dots, J_k(t)]$, with k the number of joints in the skeleton, and $J_i(t)=[x_i(t), y_i(t), z_i(t)]$ the 3D coordinates of joint i . The goal is to generate a reaction $Y=\{Y_1, Y_2, \dots, Y_T\}$ a sequence of skeleton poses from $X=\{X_1, X_2, \dots, X_T\}$ a sequence representing the action motion.

Our overall architecture of InterFormer is illustrated in Figure 2 and consists of four modules: a motion encoder, a motion decoder, a skeleton adjacency module and an interaction distance module. The motion encoder encodes the motion of the skeleton using self spatial skeleton and self temporal motion attentions. Both aim to find the important spatial and temporal relations within the input action motion to transmit them to the decoder. The motion decoder generates the reaction motion using the encoding from the motion encoder and consists of self spatial skeleton attention, self temporal motion attention, interaction spatial skeleton attention, and interaction temporal motion attention. Moreover, the skeleton adjacency and interaction distance modules help the different spatial attentions to focus on the most important parts of the skeletons and of the interaction.

A. Motion Encoder

The motion encoder takes as input an action sequence X to which we add positional encoding defined by [29]. This positional encoding encodes temporal information of each frame in the sequence. Inspired by [29] we use temporal attention to capture the temporal relationships within the motion of the skeleton. However, the motion contains both temporal and spatial information. Thus, we add a spatial attention module to complement the temporal attention to help find the spatial dependencies within the skeleton.

Self Spatial Skeleton Attention. For our self spatial skeleton attention module we consider each frame independently and look at the relation between the position of each joint. We use the scaled dot-product attention from [29]:

$$\text{Attention}(\mathbf{Q}, \mathbf{K}, \mathbf{V}) = \text{softmax}\left(\frac{\mathbf{Q}\mathbf{K}^T}{\sqrt{\dim}}\right) \mathbf{V}, \quad (1)$$

where \mathbf{Q} , \mathbf{K} , and \mathbf{V} are the query, key, and value matrices of sizes $\dim \times |P_t|$ which contain a set of queries, keys, and values (one for each joint in the skeleton for a given frame) of sizes \dim which is for spatial attention $|J_1(t)|$. These queries q_i , keys k_i , and values v_i are obtained by multiplying an input a_i , b_i , and c_i by weight matrices \mathbf{W}_q , \mathbf{W}_k , and \mathbf{W}_v of size $\dim \times \dim$:

$$q_i = a_i \mathbf{W}_q, \quad k_i = b_i \mathbf{W}_k, \quad v_i = c_i \mathbf{W}_v. \quad (2)$$

For self attention $a_i=b_i=c_i$ and for spatial attention they represent the 3D coordinates of joint i at a given time, either directly or through the value corresponding to the coordinates after going through the previous attention layers. We use the multihead version of the attention [29] where the inputs are split into smaller parts according to the input size of each head. Each part is treated by its own attention module and the outputs of these modules concatenated. For spatial attention, we fix the number of heads at $|J_1(t)|$, one for each dimension of the 3D coordinates.

Self Temporal Motion Attention. For the self temporal motion attention, we consider the entire skeleton and observe the motion of its joints over time, i.e., we try to find the links between the position of the joints from one frame to another. This is performed in the same way as for self spatial skeleton attention by using Eq. (1) and Eq. (2). However, here $a_i=b_i=c_i$ represent the entire skeleton at time $t=i$, $\dim=d$ and \mathbf{Q} , \mathbf{K} , and \mathbf{V} are of size $\dim \times T$. We also use the multihead version of the attention, but here the number of heads can be set as a hyperparameter.

B. Motion Decoder

The decoder receives the encoder’s output Z as well as the reaction sequence Y . It is composed of four attention modules as illustrated in Figure 2. The self attention modules work in the same way as for the encoder but take Y to which we add the positional encoding as input.

Interaction Spatial Skeleton Attention. The interaction spatial skeleton attention module looks at the relations between the joints of the interacting skeletons at a given frame. The attention is also computed using Eq. (1) and Eq. (2) but here

the query matrix Q comes from the reaction sequence Y and the key and value matrices K and V come from the encoder output Z .

Interaction Temporal Motion Attention. The interaction temporal motion attention module looks at the relations between the frames from the action sequence and the frames from the reaction sequence. Discovering these relations enable the synchrony of the generated reaction. Likewise the query matrix Q comes from the reaction sequence Y but the key and value matrices K and V come from the encoder output Z .

In both the encoder and decoder, before each attention module, the input is normalized, and after each module, the output is also normalized and added to a residual connection of the non-normalized module input like in [29]. The spatial and temporal attentions are computed in parallel and are added after passing through all modules. This final output then goes through a feed-forward layer and is added to the residual connection. The architectures described here for the encoder and the decoder correspond to a single layer of the encoder and one single layer of the decoder. There are $N=6$ of each of these layers, and the input of layer h is the output of layer $h-1$. Finally, after the last decoder layer, the output goes through a final linear layer to get the reaction sequence.

C. Skeleton Adjacency and Interaction Distance

Recently many works using skeletons also use a graph representation which was proved to be a particularly efficient representation for action recognition [27], [28]. Building a graph for a skeleton is particularly intuitive in that the joints of the skeletons are already linked together by body segments. However, in our case, using a graph representation might be ill-fitted. Indeed while graphs provide information about the skeleton structure and help us concentrate on the most interesting parts of the skeleton, it would limit us when modeling the interaction. The information we have about the interaction is contained in the attention between the encoder and the decoder and the relations in the skeleton graph are very different from the relations between the joints of the two skeletons (all relations are possible). However, graphs can still provide important information that we can use to improve our generation.

Skeleton Adjacency Module. We can use the information contained in the graph representation by looking at the adjacency matrices of the joints. We use three adjacency matrices that we combine to create a mask. The three matrices are based on the ones used by [28]: (i) the identity matrix I used to represent the joints themselves; (ii) the matrix of inward relations In which are the paths from the extremities (head, hands, and feet) to the root joint (torso or pelvis), and (iii) the matrix of outward relations Out which represents the paths from the root joint to the extremities. The three matrices of sizes $|P_t| \times |P_t|$ are then added to get the mask matrix $M=I+In+Out$ that we apply to the attention matrix Att of size $|P_t| \times |P_t|$ to hide values that are not part of the graph

as illustrated in the top right part of Figure 2.

$$Att_{i,j} = \begin{cases} Att_{i,j}, & \text{if } M_{i,j} \neq 0 \\ 0, & \text{if } M_{i,j} = 0 \end{cases} \quad (3)$$

Interaction Distance Module. Interaction attention, which is also the attention between the encoder and the decoder, can also use a graph representation [27], but this graph cannot be fixed since the interesting links between joints vary from class to class e.g., for “punching” we are interested in the link between the hand and the head but not for “kicking”. Ultimately, it is the spatial attention between the encoder and decoder that discovers the important links between the two skeletons. However, as suggested by [27] we can add prior knowledge to the attention to help us model the interaction for some classes. This information is the distance between the joints of both skeletons, i.e., joints that are close to each other are more likely to interact than those that are far away:

$$Dist_{i,j} = -\|J_{action}^i(t) - J_{reaction}^j(t)\|_2, \quad (4)$$

where $J_{action}^i(t)$ and $J_{reaction}^j(t)$ are the joint i and j of the action and reaction skeletons at time t , $Dist$ is a matrix of size $|P_t| \times |P_t|$. Unlike the graph for self spatial attention, we do not use the distance matrix to create a mask because some of the relations between the two skeletons are not defined by the distance between the joints (e.g., waving and waving back), thus using the distance matrix as a mask would prevent such relations from being discovered. We add $\text{softmax}(Dist)$ to the attention matrix to keep all the information that interests us, as illustrated in the top right part of Figure 2. By using the softmax function on the distance matrix, we add values of the same order to the attention matrix while making shorter distance more important.

D. Objective Optimization

We use two loss functions to direct our model. The first one is the sequence loss (L_s) which compares the generated sequence with the corresponding ground truth using the Mean Square Error (MSE) :

$$L_s = \frac{1}{T} \frac{1}{k} \sum_{t=1}^T \sum_{i=1}^k (J_i(t) - \hat{J}_i(t))^2, \quad (5)$$

where $J_i(t)$ is the position of the real joint i at time t and $\hat{J}_i(t)$ the position of the generated joint i at time t . The second is the first frames loss (L_{ff}) used to add constraints on the first two frames by ensuring that the motion between the two is realistic and limits the discontinuities that can happen at the beginning of the sequences. This loss is necessary as otherwise the model sometimes ignore the initial input frame and generate a sequence based on its own inferred initial position. For this loss, we also use the MSE but on the difference between the two first frames:

$$L_{ff} = \frac{1}{k} \sum_{i=1}^k ((J_i(2) - J_i(1)) - (\hat{J}_i(2) - \hat{J}_i(1)))^2. \quad (6)$$

E. Implementation Details

We train our InterFormer using Torch 1.8.1 on a PC with two 2.3Ghz processors, 64G RAM, and an Nvidia Quadro RTX 6000 GPU. We use the Adam optimizer [36] with $\alpha=0.0001$, $\beta_1=0.9$, $\beta_2=0.98$, and $\epsilon=1 \times 10^{-9}$. The batch sizes are set to 128 for SBU and DuetDance and 64 for K3HI. InterFormer works even if we do not provide the original position of the reaction sequence (the first frame of the sequence) as input, but this can cause the generator to produce a skeleton very far from its actual location, which will lead to a bad generation. To solve this during testing, we give as input to the decoder the first frame of the sequence which gives information about the original location of the skeleton. During testing we generate sequences of variable lengths depending on the length of the input action motion. The sequences are generated in a auto-regressive manner and the model generates an end-of-sequence value to indicate the end of the motion generation. If the motion is generated correctly, then this value will correspond to the end of the input action sequence.

IV. EXPERIMENTS

We conducted comprehensive experiments to evaluate our proposed approach by comparing state-of-the-art models on three datasets. We also visualize the ability of the action-reaction generation. Finally, we perform ablation studies to evaluate the effectiveness of using the spatial attention and our skeleton adjacency and interaction distance modules.

A. Datasets

SBU Dataset [17] contains 8 classes of simple interaction motions: walking toward, walking away, kicking, pushing, shaking hands, hugging, exchanging, and punching. The data which are too noisy, and in particular the class “hugging”, have been removed from this dataset. The “walking away” and “walking toward” classes have the same reactions (standing still), so we decided to fuse those two classes into a single “walking” class. This leaves us with 6 classes, 195 training and 30 test samples.

K3HI Dataset [37] contains the same 8 classes as SBU aside from the “hugging” class which is replaced by “pointing”. Also, unlike SBU, “approaching” and “departing” have reactions that are different, so we do not fuse the two classes. We also removed the noisy samples from the dataset but this time we normalize the data in the same way as SBU was normalized by the authors. This leaves us with 236 training samples and 28 test samples.

DuetDance Dataset [2] contains 5 classes of dance motions: cha-cha, jive, rumba, salsa, and samba. Given the nature of the dataset, the motions are more complex than those in SBU and K3HI, and there is a lot of intra-class variabilities. We do not perform normalization, but since most samples are very long sequences (up to 160s), we decided to cut each sequence into smaller sequences of 50 frames (2s), leading to 273 training samples and 3991 test samples.

For all three datasets the poses are represented by their absolute 3D coordinates, furthermore training and testing splits are selected randomly for fair comparisons. Duet-Dance was

provided with neither train/test split nor subject information, we used a random split. For the two other the evaluation proposed by their respective authors is made using k-fold validation so we decided to split the dataset between train and test, randomly for K3HI and by selecting all the sample from a random subject for SBU

B. Evaluation Metrics

We use metrics commonly used in motion generation. Metrics used for motion prediction based on the distance between the generated sample and the ground truth are not fit for reaction generation as several different motions can be considered as good reactions to the same action. While this choice of metric can seem contradictory with our losses that use direct comparison with the ground truth, it is important to understand that our evaluation metrics do not contain direct information about the skeleton that our network is supposed to generate and could not be efficiently used as losses.

Classification Accuracy measures how well our generated samples are classified by a motion classifier. We use the DeepGRU classifier [38]. We only train and test the classifier on the reaction part of the interaction, so the results are not influenced by the action, which is always the ground truth. We report the percentage of correctly classified samples for each class and the average over the entire test set.

Fréchet Video Distance (FVD) is an adaptation of the Fréchet Inception distance (FID) [39] for video sequences [40]. FVD computes the distance between the ground truth and the generated data distribution.

$$FVD = |\mu_{gt} - \mu_{gen}|^2 + \text{tr} \left[\mathbf{C}_{gt} + \mathbf{C}_{gen} - 2(\mathbf{C}_{gt} * \mathbf{C}_{gen})^{1/2} \right], \quad (7)$$

where μ_{gt} , μ_{gen} and \mathbf{C}_{gt} and \mathbf{C}_{gen} are the means and covariance matrices of the deep features from ground truth and the generated samples respectively, $\text{tr}(\cdot)$ is the trace. The deep features are obtained from the classifier used for the classification accuracy

Diversity Score. Following the metric defined by [41], [42] we compute the average deep feature distance between all the samples generated by each method and then compare it to the average deep feature distance of the ground truth. A low diversity score means that the generated samples have a diversity close to that of the ground truth and a high score means that the diversity is either lower (all motions are more similar) or higher (more noise in the generation). The average deep feature distance is calculated as follows:

$$div = \frac{1}{b(b-1)} \sum_{i=1}^b \sum_{j=1}^b \|F_i - F_j\|_2, \quad (8)$$

where b is the number of samples considered, F_i and F_j are deep features of the samples i and j , respectively. The score is obtained using div_{gt} the diversity distance of the ground truth and div_{gen} the diversity of the generated samples.

$$score = 100 \times \frac{|div_{gt} - div_{gen}|}{div_{gt}}. \quad (9)$$

C. Baselines

To our knowledge, there is no work that deals with the generation of the reaction to an action, so to be able to compare our results to others from the literature, we employ a method for human interaction generation and a method for human motion prediction to show methods used on a range of applications.

Zero Velocity baseline (ZeroV) [4] is a simple baseline where all generated frames are the same (in our case the initial pose), there is no motion for this baseline. Using ZeroV as a comparison is useful to see what the quantitative result of an obviously bad method are like and help see if the results from the other methods are actually good. We do not show the results for ZeroV in our qualitative evaluation as they are uninteresting since no motion is produced. We do not use them in our user study for the same reason.

Multimodal Variational Recurrent Neural Network (VRNN) [1] deals with the prediction of the future frames of a two-person interaction based on a historical sequence using variational RNNs. The next frame of the reaction is predicted using the past frames of the reaction and information on the past frames of the action; the action is predicted in the same way using information on the reaction. The past frames are the historical sequence at the beginning and later in the sequence the generated frames. To fit our problem, we modified their network so the reaction would have no historical sequence aside from the first frame, and the action would have the entire sequence as the historical sequence. We use the default settings provided by the author for the hyper-parameters.

Mix-and-Match Perturbation (MixMatch) [43] uses a recurrent encoder-decoder network with a conditional variational autoencoder block to predict the motion of a single person based on a historical sequence. However, the method can be used for prediction in other domains, e.g., the code they provide use the first half on an image to predict the second half. The code used for motion prediction is not available. We have adapted this network for reaction generation but unlike them we do not generate directly the 3D coordinates, computing the speed of each joint and then apply it to the first frame to get the reaction motion. We use the hyperparameters values mentioned in [43] for human motion prediction.

D. State-of-the-Art Comparisons

All presented evaluation were obtained on a model trained on the considered dataset. This is true for our InterFormer as well as the baselines.

Quantitative Evaluation. Table I (left) shows the classification accuracy for SBU, DuetDance, and K3HI. Our method outperforms the three others on all the datasets. For SBU, we obtain results very close to the ground truth, and we outperform the other methods on all classes but “exchanging” where [1] get better results and vastly outperform the simple ZeroV baseline. InterFormer is able to generate simple motions that are realistic enough to be correctly classified.

For K3HI, we can see that the results are worse than for SBU for all methods and even for the ground truth. This is due to the very noisy nature of the K3HI dataset even after

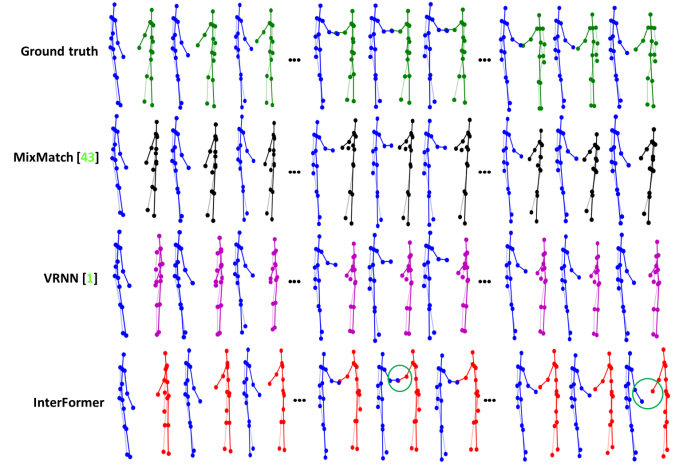


Fig. 3: **Qualitative results.** In blue the action motion used as a condition, in other colors the reaction either from the ground truth or generated by the different models. Shaking hands class from the SBU dataset.

removing the worse samples (that showed extreme deformation and no recognizable motion), the exchanging class has a 0% recognition rate even for the ground truth. However, our method provides better results than the two others on all classes except “approaching” which may be due to the noisy nature of the data for this class. VRNN obtaining very high results on this class might be a consequence of the wrong classification present on many of the classes (a lot of samples are classified as approaching).

For DuetDance, the classification accuracy for all methods and the GT is much closer than for the other datasets. This is due to the complex motions contained in the dataset with a lot of intra class variability. Furthermore, we use sequences of 50 frames which are short enough that some sequences from two different classes can be very similar. We can still notice that our method provides results that are the closest to the ground truth and that, unlike the two other methods no class has a score below chance (i.e., 20%) which mean that our results are more consistent and closer to the ground truth.

In Table II we show the FVD and diversity score for all methods on all datasets. We outperform VRNN and MixMatch on the FVD measure, often by a large margin meaning that the features extracted by the classifier are closer to the features of the ground truth than for [1] and [43]. For the diversity score, we also outperform the two other methods and provide diversity that is close to that of the ground truth. We can see a significant increase in K3HI. This is due to the noisy nature of the dataset, which means that the diversity distance of the ground truth takes into account the noise of the sample, we however manage to score the closest to the diversity of the ground truth when compared to the other methods, without generating noisy samples.

User Study. To evaluate the quality of the generated videos, we also conduct a user study. Specifically, the users are given four videos (two generated by existing methods VRNN and MixMatch, one generated by our proposed InterFormer, and one real video) with the corresponding class label, each participant needs to answer one questions: ‘Which video is more realistic regardless of the input label?’. 20 users have

TABLE I: **Left:** Classification accuracy for each classes of the SBU, DuetDance, and K3HI datasets. **Right:** User study for each classes of the SBU, DuetDance, and K3HI datasets.

Method	GT	ZeroV [4]	VRNN [1]	MixMatch [43]	InterFormer	GT	VRNN [1]	MixMatch [43]	InterFormer
Classification Accuracy \uparrow						User Preference \uparrow			
SBU									
Walking	100.0	0.0	58.3	100.0	100.0	34.2%	21.4%	15.5%	28.9%
Kicking	66.7	66.7	0.0	0.0	33.3	38.8%	23.8%	5.6%	31.8%
Pushing	80.0	0.0	60.0	0.0	60.0	35.6%	19.7%	15.4%	29.3%
Shaking Hands	100.0	0.0	0.0	0.0	100.0	37.5%	21.8%	7.8%	32.9%
Exchanging	80.0	0.0	80.0	0.0	60.0	41.9%	19.4%	13.0%	25.7%
Punching	100.0	33.3	0.0	33.3	100.0	43.1%	19.3%	11.3%	26.3%
Average	90.0	10.0	46.7	43.3	80.0	38.5%	20.9%	11.4%	29.2%
DuetDance									
Cha-Cha	28.0	1.8	26.4	19.2	26.7	45.9%	17.8%	5.5%	30.8%
Jive	24.6	0.4	13.8	25.8	22.8	48.4%	13.2%	6.7%	31.7%
Rumba	34.8	0.7	36.4	30.0	32.0	40.7%	16.9%	8.2%	34.2%
Salsa	27.8	93.1	29.5	28.9	28.1	49.3%	12.8%	7.1%	30.8%
Samba	22.2	18.6	21.0	17.2	24.4	44.5%	15.8%	6.3%	33.6%
Average	28.0	24.6	26.2	24.9	27.1	45.8%	15.3%	6.7%	32.2%
K3HI									
Approaching	100.0	25.0	75.0	50.0	0.0	34.9%	23.1%	14.1%	27.9%
Departing	33.3	33.3	0.0	33.3	33.3	34.2%	24.2%	13.2%	28.4%
Kicking	40.0	80.0	0.0	40.0	60.0	31.8%	21.7%	18.8%	27.7%
Pushing	100.0	33.3	33.3	33.3	66.7	33.1%	24.8%	13.5%	28.6%
Shaking	50.0	0.0	50.0	50.0	50.0	36.9%	21.4%	10.8%	30.9%
Exchanging	0.0	0.0	0.0	0.0	0.0	36.3%	20.5%	13.9%	29.3%
Punching	100.0	25.0	50.0	25.0	50.0	33.9%	21.7%	16.9%	27.5%
Pointing	100.0	50.0	100.0	0.0	100.0	37.3%	20.2%	16.1%	26.4%
Average	67.9	35.7	39.3	28.6	46.4	34.8%	22.2%	14.7%	28.3%

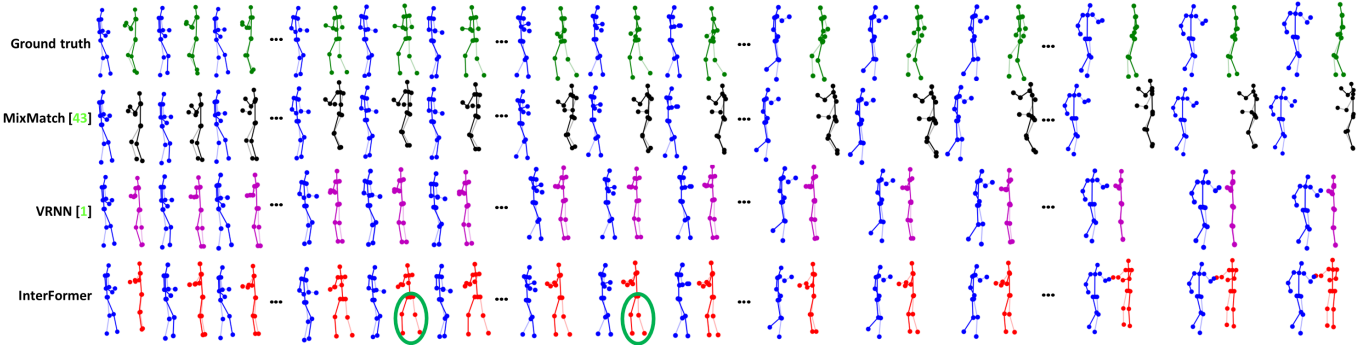


Fig. 4: **Qualitative results.** In blue the action motion used as a condition, in other colors the reaction either from the ground truth or generated by the different models. Cha-cha class from the DuetDance dataset.

TABLE II: FVD and diversity on all datasets.

Method	FVD \downarrow			Diversity \downarrow		
	SBU	DuetDance	K3HI	SBU	DuetDance	K3HI
ZeroV [4]	493.3	41058.1	392.1	65.1	47.2	19.3
VRNN [1]	113.61	789.23	195.47	11.5	6.1	16.8
MixMatch [43]	314.38	1460.44	406.63	45.3	0.9	32.2
InterFormer (Ours)	48.78	31.81	125.40	0.9	0.4	13.7

TABLE III: Ablation study of Interformer on the SBU dataset.

	Setup	Accuracy \uparrow	Diversity \downarrow
S1	Transformer	53.3	9.5
S2	S1 + Spatial Attention	66.7	3.9
S3	S2 + Skeleton Adjacency	73.3	1.7
S4	S3 + Interaction Distance	80.0	0.9

unlimited time to select their choices. The results are shown in Table I (right), we can see that the users show more preference for our method than the other two methods, which indicates the results generated by ours are more realistic.

Qualitative Evaluation.

We show in Figure 3 Figure 6, Figure 4 and Figure 5 visualizations of the generated sequences on the SBU (two sequences) DuetDance and K3HI datasets respectively. We

show from top to bottom: the ground truth, results for [43], result from [1], and results from our InterFormer. In blue is the action motion which serves as a condition and is in all cases the ground truth. In green, black, magenta and red are the reactions for the GT and the three methods. More visualizations as well as animations are available in our supplementary materials.

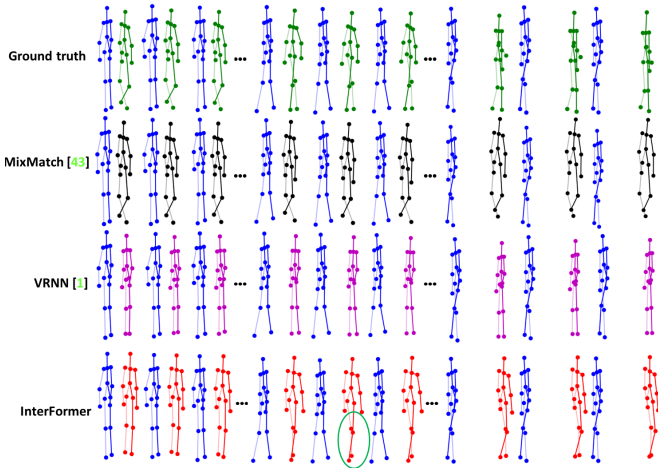


Fig. 5: **Qualitative results.** In blue the action motion used as a condition, in other colors the reaction either from the ground truth or generated by the different models. Departing class from the K3HI dataset.

In Figure 3 we show an interaction from the “shaking hands” class of SBU. It shows that our method is able to generate the motion better than the two other methods. For [43], the character raises its hand to shake but never comes really close to the other character’s hand and also shifts its entire body backward toward the end of the sequence. [1] generates a motion that raises slightly the hand but is then stuck in this position. Our method generates motion that is very close to the ground truth and contains the three main steps of the motion: raising the hand, shaking, and going back to starting position. Figure 6 shows a sample from the “punching” class from the SBU dataset. We see that we generate a better motion even if there are differences with the ground truth. The character is pushed to the side by the punch and then comes back to a normal position at the end of the sequence. The two other methods also generate a reaction to the punch, [1] moves slightly backward and [43] move its upper body to avoid the punch. It seems, however, that the upper body also became smaller during this motion. The two methods also stay in this avoiding pose and do not go back to a more normal position. In Figure 4 we show a sample of the “cha-cha” class from the challenging DuetDance dataset. We can see that [43] produce a motion that resembles a dance even if different from the ground truth, however as the action character moves backward (better seen in the animated sequence in our supplementary material), the generated reaction stays in place, and the distance between both characters grows over time. With [1] the distance between the two characters does not grow, but there is barely any motion for the entire sequence. In motion, it looks like the reaction character is gliding toward the action character (better seen in the animation in our supplementary material). Our method is able to generate a motion that stays close to the ground truth and follows the action character in space without gliding like [1] this can be seen by the change of position of the legs across the sequence. It is only toward the end that the motion differs from the ground truth and even then, the motion still resembles dancing.

In Figure 5, we see a sample of the departing class from

the K3HI dataset. It shows both characters walking away from each other. This behavior is always reproduced in the samples generated by the three methods, but [1] does not show much motion and simply glide away while [43] show more motion of the legs but keep the noise present in the first frame during the entire sequence. Our method, on the other hand, generates a realistic walking motion with both arms and legs moving to move apart from the first character.

Multi-Modality Generation. The main issue of Transformer models is that their output is deterministic. To counter this we can add noise to the encoder input before the first feed-forward layer. This allows us to generate diverse outputs for the same input motion. We show in Figure 7 and Figure 8 the ability of our method to generate diverse motions with a single input when adding noise in the encoder.

E. Ablation Study

To validate the effectiveness of each proposed component, we report the ablation studies on SBU with classification accuracy and diversity.

Ablation Models. Our InterFormer has four versions (i.e., S1, S2, S3, S4) as shown in Table III. (i) S1 means only using the original NPL Transformer network from [29] modified to take as input and generate skeletons without any of our improvements. (ii) S2 adds to the global Transformer the spatial attention modules (self spatial attention and interaction spatial attention). (iii) S3 adds the skeleton adjacency module to the self spatial attention. (iv) S4 is the full model and includes both the skeleton adjacency module and the interaction distance module.

Effect of Spatial Attention. We validate the effect of the spatial attention, as shown in Table III. Introducing the spatial attention results in significant improvement in classification accuracy by 13% and the diversity by 5.6, which means we improve the quality of the action-reaction sequences.

Effect of Skeleton Adjacency. Using a skeleton adjacency graph on attention improves the classification accuracy and diversity by 7% and 2.2, respectively. This improvement means that the model learns better relations between the different joints inside a skeleton.

Effect of Interaction Distance. By adding the interaction distance module, we increase the results obtained by the skeleton adjacency module by 7% on classification and 0.8 on diversity. These results show that the interaction distance module is able to help spatial interaction attention find the most interesting relations between the two skeletons and thus help generate better motions.

Effect of Loss on The First Frames. If we remove the loss on the first frames that allow us to keep a good coherency between the input initial position and the generation we see a decrease in the generation quality: -3.3% in classification accuracy and -5.2 in diversity score when compared to S4. When the input initial position is not properly taken into account the generated reaction skeleton can be far from the action skeleton. In SBU for all action classes the interactions consist of two persons close to each other. Since the model is not trained with samples where people are far from each other when we try to generate

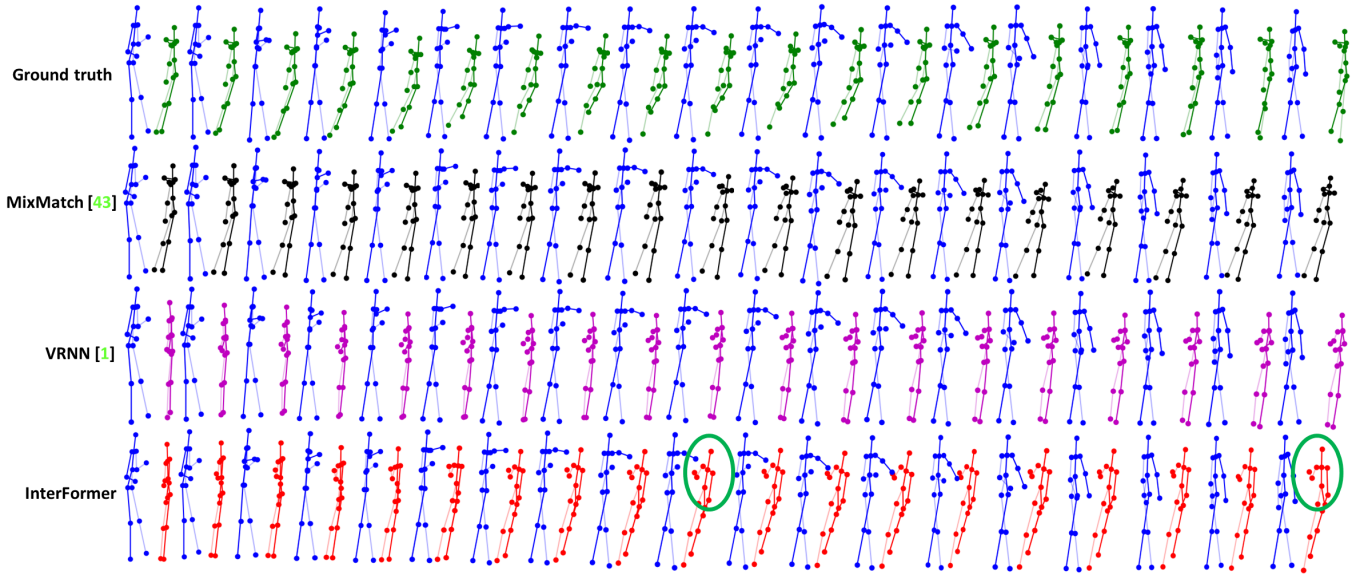


Fig. 6: **Qualitative results.** In blue the action motion used as a condition, in other colors the reaction either from the ground truth or generated by the different models. Punching class from the SBU dataset.

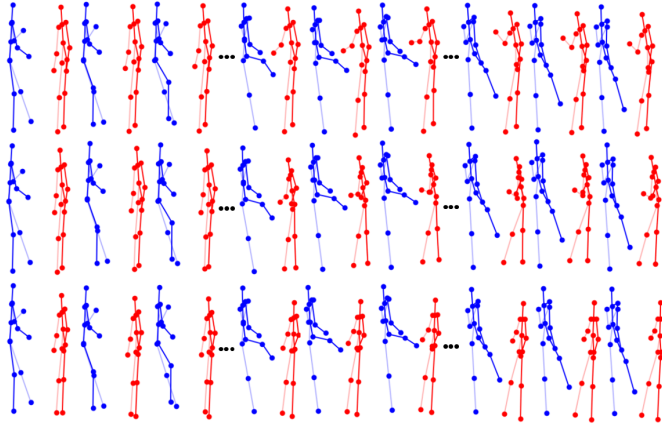


Fig. 7: **Multi-modality results on SBU kicking class with noise.** We show three different motions generated by our Interformer based on the same input motion.

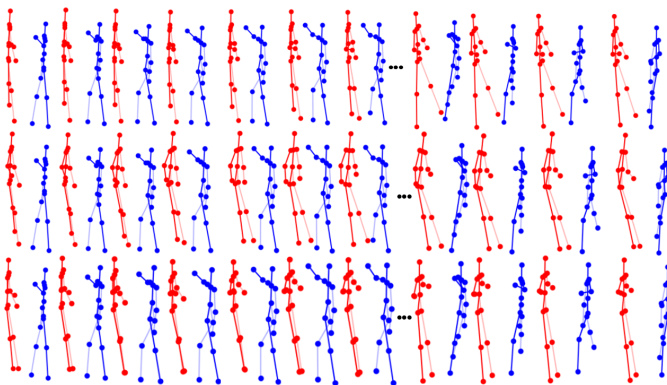


Fig. 8: **Multi-modality results on SBU Punching class with noise.** We show three different motions generated by our Interformer based on the same input motion.

the reaction motion of a skeleton far from the action skeleton little to no motion is generated. This explain the increase in performance brought by the use of the first frame loss.

Effect of Multihead attention. Our Interformer uses the

T multihead	S multihead	Accuracy \uparrow	Diversity \downarrow
-	-	60.0	10.6
✓	-	70.0	2.0
-	✓	60.0	5.1
✓	✓	80.0	0.9

TABLE IV: Ablation study of Interformer on the SBU dataset.

multihead version of attention for both temporal and spatial attention. These choices were made following results from the original Transformer network [29] and our experiments which we report in Table IV. The results are obtained by modifying the number of head for the different attentions modules on the full Interformer model (S4 from the main paper ablation study). These experiments show that using the multihead temporal attention (T multihead) increase the classification accuracy by 10% and diversity by 8.6. By using only the spatial multihead attention (S multihead) we increase the diversity 5.5. Using the multihead attention for both spatial and temporal attention lead to an increase of 20% in classification accuracy and 9.7 in diversity. This confirms our choice to use this configuration for Interformer.

V. LIMITATIONS

InterFormer presents two main limitations: (i) Due to the huge variability of complex motions, it is hard to stay true to the ground truth, making it difficult to evaluate the results in these cases; (ii) We are able to generate realistic motion for long sequences (tested up to 40 seconds) To do this we cut the action sequence in smaller sub-sequences that we use for generation. We then generate all these sequences the same way as we do for shorter sequences. Only for the second sub-sequence onward the first frame used to give the initial position does not come from ground truth but instead is the last generated frame from the previous sub-sequence. We can see in “DuetDance-long.mp4” from our supplementary material that this way InterFormer is able to generate reaction sequence

for long motion. However due to the accumulation of error over time, the generation diverges more and more from the ground truth up to the point where it is hard to know how much the action is taken into account in the generation. It is even more true that very long motions are usually complex ones, which mean we also face the first limitation.

VI. CONCLUSION

We present InterFormer, a novel human reaction generation Transformer. InterFormer is the first Transformer architecture used to solve the problem of human reaction generation challenge. InterFormer consists of four modules: a motion encoder, a motion decoder, a skeleton adjacency module, and an interaction distance module. The ablation study on SBU has shown the effectiveness of the four components of the InterFormer. We have both qualitatively and quantitatively evaluated our reaction generation framework. The results show that InterFormer outperforms state-of-the-art approaches in terms of FVD, classification, and diversity score on three challenging datasets SBU, K3HI, and DuetDance. The qualitative results show also the ability of InterFormer to generate realistic human reactions.

REFERENCES

- [1] M. Baruah and B. Banerjee, "A multimodal predictive agent model for human interaction generation," in *CVPR Workshops*, 2020. **1, 2, 6, 7, 8**
- [2] J. Kundu, H. Buckchash, P. Mandikal, R. M. V. A. Jamkhandi, and R. Babu, "Cross-conditioned recurrent networks for long-term synthesis of inter-person human motion interactions," in *WACV*, 2020. **1, 2, 5**
- [3] A. Kacem, M. Daoudi, B. B. Amor, S. Berretti, and J. C. Alvarez Paiva, "A novel geometric framework on gram matrix trajectories for human behavior understanding," *IEEE Trans. Pattern Anal. Mach. Intell.*, vol. 42, no. 1, pp. 1–14, 2020. **2**
- [4] J. Martinez, M. J. Black, and J. Romero, "On human motion prediction using recurrent neural networks," in *CVPR*, 2017. **2, 6, 7**
- [5] Q. Cui, H. Sun, and F. Yang, "Learning dynamic relationships for 3D human motion prediction," in *CVPR*, 2020. **2**
- [6] M. Devanne, H. Wannous, S. Berretti, P. Pala, M. Daoudi, and A. Del Bimbo, "3-D human action recognition by shape analysis of motion trajectories on Riemannian manifold," *IEEE Trans. Cybernetics*, vol. 45, no. 7, pp. 1340–1352, 2014. **2**
- [7] K. Fragkiadaki, S. Levine, P. Felsen, and J. Malik, "Recurrent network models for human dynamics," in *ICCV*, 2015. **2**
- [8] R. Zhao, H. Su, and Q. Ji, "Bayesian adversarial human motion synthesis," in *CVPR*, 2020. **2**
- [9] Z. Wang, P. Yu, Y. Zhao, R. Zhang, Y. Zhou, J. Yuan, and C. Chen, "Learning diverse stochastic human-action generators by learning smooth latent transitions," in *AAAI*, 2020. **2**
- [10] Y. Zhou, Z. Li, S. Xiao, C. He, Z. Huang, and H. Li, "Auto-conditioned recurrent networks for extended complex human motion synthesis," in *ICLR*, 2018. **2**
- [11] R. Li, S. Yang, D. A. Ross, and A. Kanazawa, "Ai choreographer: Music conditioned 3d dance generation with AIST++," *ICCV*, pp. 13 381–13 392, 2021. **2**
- [12] W. Yin, H. Yin, D. Kragic, and M. Björkman, "Graph-based normalizing flow for human motion generation and reconstruction," 2021. **2**
- [13] C. Ahuja, D. W. Lee, R. Ishii, and L.-P. Morency, "No gestures left behind: Learning relationships between spoken language and freeform gestures," in *EMNLP*, 2020. **2**
- [14] I. Habibie, W. Xu, D. Mehta, L. Liu, H.-P. Seidel, G. Pons-Moll, M. Elgharib, and C. Theobalt, "Learning speech-driven 3d conversational gestures from video," in *ACM International Conference on Intelligent Virtual Agents (IVA)*, 2021. **2**
- [15] T. Sofianos, A. Sampieri, L. Franco, and F. Galasso, "Space-time-separable graph convolutional network for pose forecasting," in *Proceedings of the IEEE/CVF International Conference on Computer Vision (ICCV)*, October 2021, pp. 11 209–11 218. **2**
- [16] J. Liu, A. Shahroudy, M. Perez, G. Wang, L.-Y. Duan, and A. Kot, "Ntu rgb+d 120: A large-scale benchmark for 3d human activity understanding," *IEEE Transactions on Pattern Analysis and Machine Intelligence*, pp. 1–18, 2019. **2**
- [17] K. Yun, J. Honorio, D. Chattopadhyay, T. L. Berg, and D. Samaras, "Two-person interaction detection using body-pose features and multiple instance learning," in *CVPR Workshops*, 2012. **2, 5**
- [18] G. Lee, Z. Deng, S. Ma, T. Shiratori, S. Srinivasa, and Y. Sheikh, "Talking with hands 16.2m: A large-scale dataset of synchronized body-finger motion and audio for conversational motion analysis and synthesis," in *ICCV*, 2019. **2**
- [19] H. Joo, T. Simon, M. Cikara, and Y. Sheikh, "Towards social artificial intelligence: Nonverbal social signal prediction in a triadic interaction," in *CVPR*, 2019. **2**
- [20] A. Gupta, J. Johnson, L. Fei-Fei, S. Savarese, and A. Alahi, "Social GAN: Socially acceptable trajectories with generative adversarial networks," in *CVPR*, 2018. **2**
- [21] C. Ahuja, S. Ma, L.-P. Morency, and Y. Sheikh, "To react or not to react: End-to-end visual pose forecasting for personalized avatar during dyadic conversations," in *ICMI*, 2019. **2**
- [22] Y. Yang, J. Yang, and J. Hodgins, "Statistics-based motion synthesis for social conversations," in *SIGGRAPH*, 2020. **2**
- [23] Y. Yoon, B. Cha, J.-H. Lee, M. Jang, J. Lee, J. Kim, and G. Lee, "Speech gesture generation from the trimodal context of text, audio, and speaker identity," *ACM Trans. Graph.*, vol. 39, no. 6, 2020. **2**
- [24] X. Qi, R. Liao, J. Jia, S. Fidler, and R. Urtasun, "3d graph neural networks for rgb-d semantic segmentation," in *CVPR*, 2017. **2**
- [25] C. R. Qi, H. Su, K. Mo, and L. J. Guibas, "Pointnet: Deep learning on point sets for 3d classification and segmentation," in *CVPR*, 2017. **2**
- [26] W. Norcliffe-Brown, E. Vafeias, and S. Parisot, "Learning conditioned graph structures for interpretable visual question answering," in *NeurIPS*, 2018. **2**
- [27] L. Zhu, B. Wan, C. Li, G. Tian, Y. Hou, and K. Yuan, "Dyadic relational graph convolutional networks for skeleton-based human interaction recognition," *Pattern Recognition*, vol. 115, 2021. **2, 4**
- [28] C. Plizzari, M. Cannici, and M. Matteucci, "Skeleton-based action recognition via spatial and temporal transformer networks," *CVIU*, vol. 208–209, p. 103219, 2021. **2, 3, 4**
- [29] A. Vaswani, N. Shazeer, N. Parmar, J. Uszkoreit, L. Jones, A. N. Gomez, L. Kaiser, and I. Polosukhin, "Attention is all you need," in *NeurIPS*, 2017. **3, 4, 8, 9**
- [30] R. Al-Rfou, D. Choe, N. Constant, M. Guo, and L. Jones, "Character-level language modeling with deeper self-attention," in *AAAI*, 2019. **3**
- [31] J. Devlin, M. Chang, K. Lee, and K. Toutanova, "BERT: pre-training of deep bidirectional transformers for language understanding," in *NAACL-HLT*, 2019. **3**
- [32] N. Parmar, A. Vaswani, J. Uszkoreit, L. Kaiser, N. Shazeer, A. Ku, and D. Tran, "Image transformer," in *ICML*, 2018. **3**
- [33] N. Carion, F. Massa, G. Synnaeve, N. Usunier, A. Kirillov, and S. Zagoruyko, "End-to-end object detection with transformers," in *ECCV*, 2020. **3**
- [34] R. Ranftl, A. Bochkovskiy, and V. Koltun, "Vision transformers for dense prediction," *ArXiv preprint*, 2021. **3**
- [35] P. Esser, R. Rombach, and B. Ommer, "Taming transformers for high-resolution image synthesis," in *CVPR*, 2021. **3**
- [36] D. Kingma and J. Ba, "Adam: A method for stochastic optimization," *ICLR*, 12 2014. **5**
- [37] T. Hu, X. Zhu, and W. Guo, "Two-person interaction recognition based on key poses," *Journal of Computational Information Systems*, vol. 10, pp. 1965–1972, 2014. **5**
- [38] M. Maghoumi and J. J. LaViola, "Deepgru: Deep gesture recognition utility," in *Advances in Visual Computing*, 2019. **5**
- [39] M. Heusel, H. Ramsauer, T. Unterthiner, B. Nessler, and S. Hochreiter, "Gans trained by a two time-scale update rule converge to a local nash equilibrium," in *NeurIPS*, 2017. **5**
- [40] T. Unterthiner, S. van Steenkiste, K. Kurach, R. Marinier, M. Michalski, and S. Gelly, "Towards accurate generative models of video: A new metric & challenges," *arXiv preprint arXiv:1812.01717*, 2018. **5**
- [41] H.-Y. Lee, X. Yang, M.-Y. Liu, T.-C. Wang, Y.-D. Lu, M.-H. Yang, and J. Kautz, "Dancing to music," in *NeurIPS*, 2019. **5**
- [42] R. Zhang, P. Isola, A. A. Efros, E. Shechtman, and O. Wang, "The unreasonable effectiveness of deep features as a perceptual metric," in *CVPR*, 2018. **5**
- [43] S. Aliakbarian, F. S. Saleh, M. Salzmann, L. Petersson, and S. Gould, "A stochastic conditioning scheme for diverse human motion prediction," in *ICCV*, 2020. **6, 7, 8**